On the Modeling of Highly Nonlinear Circuits Using Total-Variation-Decreasing Finite-Difference Schemes

Werner Thiel and Wolfgang Menzel, *Fellow, IEEE*

***Abstract*—This paper presents the modeling of highly nonlinear circuits using a total-variation-decreasing (TVD) difference scheme developed for the simulation of problems involving shock phenomena. In contrast to the commonly used leapfrog scheme, a second-order accurate TVD method based on the Lax–Wendroff scheme is applied to one-dimensional nonlinear transient electromagnetic-wave problems. Furthermore, for the analysis of transmission-line-based networks, an adapted inclusion of nonlinear lumped elements in such a TVD scheme is proposed. As an example, both the scattered signals of a linear transmission line loaded with a nonlinear lumped element is investigated and the formation of a shock-wave of a low-loss nonlinear transmission line with distributed diodes is studied. In the simulation results, the modeling of rapidly rising edges occurring in the time signal are demonstrated.**

***Index Terms*—Finite-difference methods, lumped-element microwave circuits, nonlinear wave propagation, TVD scheme.**

I. Introduction

A GREAT advantage of time-domain methods is the possibility to model many kinds of nonlinear microwave structures. That is one of the reasons why they have become more and more popular over the last few years. However, in highly nonlinear circuits where the time signal contains steep edges or even a discontinuity, problems emerge with the commonly used second-order accurate leapfrog scheme for electromagnetic wave phenomena, e.g., the Yee scheme in the three-dimensional (3-D) case. This class of numerical schemes only produces good results if the time signal is smooth enough. If the fall or rise times of the signal comes into the range of a few time steps only, an oscillation of the signal can be observed in the vicinity of the edge due to the numerical dispersion.

Steep edges in the time signal are mainly caused by nonlinear lumped elements included in the circuit. For this case, in [1], a solution was suggested to avoid the overshoot phenomena and a subsequent ringing of the signal. In [1], an adaptive time step depending on the slope of the signal was proposed, but this approach can only be successful if the effect of the nonlinearity is reduced by parasitic and ohmic effects so that a jump in the signal can never occur.

In this paper, a second-order accurate total-variation-decreasing (TVD) scheme [2] based on the Lax–Wendroff scheme [3] is used to describe the propagation of signals containing steep edges or even discontinuities. TVD methods originally have been developed for 25 years for conservation laws, e.g., in fluid dynamics, involving shock phenomena, and now, multidimensional higher order accurate schemes [4] are available for systems of conservation laws and can be applied to many kind of problems, not necessarily to fluid dynamics. In Section II, the basic principles and construction of TVD schemes are explained for one-dimensional (1-D) conservation laws. In Section III, the scheme is applied to a 1-D linear transmission line, which was presented in [5] first, basically showing the propagation of a step function. Next, a method for the inclusion of nonlinear elements in the transmission line is developed, preserving the TVD condition, and boundary conditions for the TVD schemes are discussed. Finally, a low-loss nonlinear transmission line (NLTL) with distributed diodes is modeled using a TVD scheme so that the shock-wave formation on the line and finally the shock-wave propagation can clearly be observed.

II. TVD Scheme

In this section, a second-order accurate TVD scheme for 1-D hyperbolic systems of conservation laws given by

$$\frac{\partial \boldsymbol{u}}{\partial t} + \frac{\partial \mathbf{F}(\boldsymbol{u})}{\partial x} = 0 \tag{1}$$

is considered, where $\boldsymbol{u} = (u_1, \ldots, u_K)^{\mathrm{T}}$, and $\mathbf{F}(\boldsymbol{u})$ is a nonlinear vector function. The system is called hyperbolic if all eigenvalues λ_i of the Jacobian matrix $\mathbf{A}(\boldsymbol{u}) = \partial \mathbf{F}(\boldsymbol{u})/\partial \boldsymbol{u}$ are real. The system of conservation laws (1) can be approximated by the difference scheme

$$\boldsymbol{u}_k^{n+1} = \boldsymbol{u}_k^n - R\left(\boldsymbol{h}_{k+1/2}^n - \boldsymbol{h}_{k-1/2}^n\right) \tag{2}$$

with $R = \Delta t/\Delta x$. In this difference equation, the numerical flux $\boldsymbol{h}_{k+1/2}^n = \boldsymbol{h}(\boldsymbol{u}_{k-q}, \ldots, \boldsymbol{u}_k, \ldots, \boldsymbol{u}_{k-p})$ generally depends on $q+p+1$ grid points. If $\boldsymbol{u}$ is a solution to conservation law (1), and if the vectors $\boldsymbol{u}_{k-j}$ with $j \in [q,p]$ in the numerical flux function are replaced by the solution $\boldsymbol{u}$, then the numerical scheme (2) is said to be consistent with conservation law (1) if $\boldsymbol{h}(\boldsymbol{u}, \ldots, \boldsymbol{u}) = \mathbf{F}(\boldsymbol{u})$.

Manuscript received October 24, 2000.

W. Thiel was with the Microwave Techniques Department, University of Ulm, D-89069 Ulm, Germany. He is now with the Department of Electrical Engineering, Radiation Laboratory, The University of Michigan at Ann Arbor, Ann Arbor, MI 48109 USA.

W. Menzel is with the Microwave Techniques Department, University of Ulm, D-89069 Ulm, Germany.

Publisher Item Identifier S 0018-9480(01)07588-3.

In the scalar case, the total variation

$$\mathrm{TV}(u^n) = \sum_{k=-\infty}^{\infty} \left|\delta_+ u_k^n\right| \tag{3}$$

of any weak solution of the system of conservation laws (1) does not increase with the time [4]. As a consequence, the numerical scheme for conservation law (1) also has to satisfy this property. A numerical scheme is TVD if the condition

$$\mathrm{TV}\left(u^{n+1}\right) \le \mathrm{TV}\left(u^n\right) \tag{4}$$

holds. This means that the numerical scheme will not increase the number of existing maxima in the function $\boldsymbol{u}$ at any time. In Section III, the evolution of the total variation over the time and the effect of the TVD criterion on a rectangular signal are studied as the example of a linear transmission line. As TVD schemes are, at most, first-order [2], a numerical scheme has to be constructed that shows an accuracy of second order at most places, especially in smooth regions, and is first-order accurate near discontinuities. Applying the flux-limiter method, the numerical flux can be composed by a low-order scheme and a high-order scheme and can be expressed by

$$\boldsymbol{h}_{k+1/2}^n = \boldsymbol{h}_{L,k+1/2}^n + \Phi_k^n \left[\boldsymbol{h}_{H,k+1/2}^n - \boldsymbol{h}_{L,k+1/2}^n\right] \tag{5}$$

where Φ_k^n represents a nonlinear function not yet determined. It can easily be seen that the low-order scheme is obtained if Φ_k^n is set to zero. In the other case, for $\Phi_k^n = 1$, a high-order scheme results. Here, as described in [2], an upwind scheme (first-order and TVD) is used for the low-order scheme, and the Lax–Wendroff (second-order) scheme is taken for the high-order scheme. Following this approach, the numerical flux can be given by

$$\boldsymbol{h}_{k+1/2}^n = \boldsymbol{h}_{L,k+1/2}^n + \frac{1}{2}\sum_{j=1}^{K} \lambda_{jk}\Phi_{jk}^n \left[\mathrm{sign}(\lambda_{jk}) - \lambda_{jk}R\right]\alpha_{jk}\boldsymbol{r}_{jk} \tag{6}$$

with

$$\boldsymbol{h}_{L,k+1/2}^n = \frac{1}{2}\left(\mathbf{F}_{k+1}^n + \mathbf{F}_k^n\right) - \frac{1}{2}\left|\hat{\mathbf{A}}\left(\boldsymbol{u}_k^n, \boldsymbol{u}_{k+1}^n\right)\right|\delta_+\boldsymbol{u}_k^n \tag{7}$$

and the smoothness parameter

$$\Theta_{jk}^n = \begin{cases} \dfrac{\alpha_{jk-1}}{\alpha_{jk}}, & \text{for } \lambda_{jk} > 0 \\ \dfrac{\alpha_{jk+1}}{\alpha_{jk}}, & \text{for } \lambda_{jk} < 0. \end{cases} \tag{8}$$

which is an indicator for the change of the slope between adjacent grid nodes. In the nonlinear case, where the Jacobian matrix $\hat{\mathbf{A}}\left(\boldsymbol{u}_k^n, \boldsymbol{u}_{k+1}^n\right)$ is not constant and depends on both space and time, some sort of average between the vectors $\boldsymbol{u}_k^n$ and $\boldsymbol{u}_{k+1}^n$ has to be chosen. According to [6], the matrix $\hat{\mathbf{A}}$ has to fulfill the following three conditions.

1) $\hat{\mathbf{A}}\left(\boldsymbol{u}_k^n, \boldsymbol{u}_{k+1}^n\right)\left(\boldsymbol{u}_{k+1}^n - \boldsymbol{u}_k^n\right) = \mathbf{F}\left(\boldsymbol{u}_{k+1}^n\right) - \mathbf{F}\left(\boldsymbol{u}_k^n\right)$.
2) $\hat{\mathbf{A}}\left(\boldsymbol{u}_k^n, \boldsymbol{u}_{k+1}^n\right)$ is diagonalizable with real eigenvalues.
3) $\hat{\mathbf{A}}\left(\boldsymbol{u}_k^n, \boldsymbol{u}_{k+1}^n\right) \to \partial\mathbf{F}(\boldsymbol{u})/\partial\boldsymbol{u}$ as $\boldsymbol{u}_k^n, \boldsymbol{u}_{k+1}^n \to \boldsymbol{u}$.

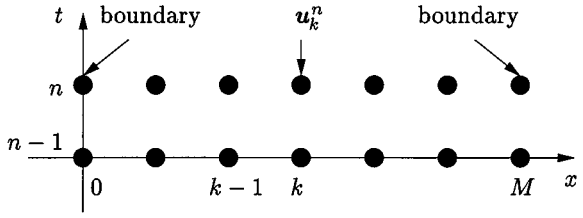

Fig. 1. Numerical domain of the TVD scheme.

Furthermore, for the calculation of the numerical flux $\boldsymbol{h}_{k+1/2}^n$ in (6), the eigenvalues λ_{jk} and eigenvectors $\boldsymbol{r}_{jk}$ have to be computed on each grid point and time step. Next, the difference vector $\delta_+\boldsymbol{u}_k^n$ has to be expanded in terms of the eigenvectors

$$\mathcal{R}\begin{bmatrix} \alpha_{1k} \\ \vdots \\ \alpha_{Kk} \end{bmatrix} = \delta_+\boldsymbol{u}_k^n. \tag{9}$$

This decomposition in terms of eigenvectors is required by the first-order upwind scheme where the spatial discretization depends on the sign of the corresponding eigenvector. Finally, the function $\Phi\left(\Theta_{jk}^n\right)$ has to be chosen in such a way that the TVD condition (4) is satisfied for all values of Θ. In the literature, several functions are proposed. In this paper, the Superbee limiter [7] is used, which can be expressed in the following way:

$$\Phi = \max\left\{0, \min[1, 2\Theta], \min[2, \Theta]\right\}. \tag{10}$$

One of the most important properties of this limiter function is the capability to sharpen the edges of the signal, which is very useful when dealing with step functions.

Finally, the TVD scheme (2) with the flux defined in (6) is considered in the numerical domain, as shown in Fig. 1. In contrast to the leapfrog scheme, all elements of the vector $\boldsymbol{u}$ are placed on the grid nodes and are computed only for whole-number time steps $n\Delta t$. Due to this arrangement, a boundary condition for all variables has to be used at the outer nodes and, therefore, the implementation of a boundary condition will differ from that of the leapfrog scheme. An absorbing boundary condition (ABC) in the case of such condensed nodes is given in Section IV. In this paper, the TVD scheme is applied to a linear and an NLTL problem. The numerical results are compared with the widely used leapfrog scheme, which is known as the Yee scheme [8] in the 3-D case. To point out the significant differences between both schemes, for a 1-D two system of conservation laws, the numerical domain of the second-order accurate leapfrog scheme of a linear transmission line (Fig. 2)

$$i_{k+1/2}^{n+1/2} = i_{k+1/2}^{n-1/2} - \frac{R}{L}\left(u_{k+1}^n - u_k^n\right) \tag{11}$$

$$u_k^{n+1} = u_k^n - \frac{R}{C}\left(i_{k-1/2}^{n+1/2} - i_{k+1/2}^{n+1/2}\right) \tag{12}$$

with the capacitance per length C, the inductance per length L, and $R = \Delta t/\Delta x$ is shown in Fig. 3. Here, the voltage u is placed on grid nodes and is updated for whole-number time steps, whereas the current i is located between two grid nodes and is computed for intermediate time steps. As a consequence

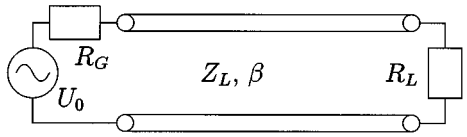

Fig. 2. Linear transmission line.

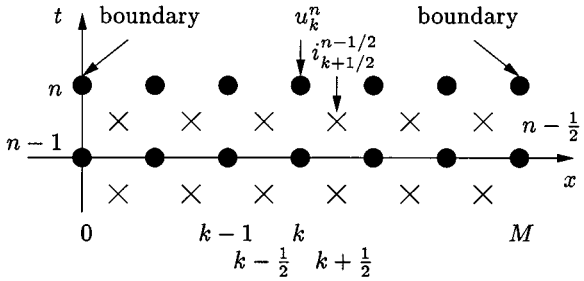

Fig. 3. Numerical domain of the leapfrog scheme.

of interleaving the components i and u of the vector $\boldsymbol{u}$, either the voltage or the current terminates the transmission line so that a different approach for a boundary condition is necessary.

III. Linear Transmission Line

As a first example, the above-described TVD scheme is applied to a lossless linear transmission line according to Fig. 2. For the first time, a TVD scheme was used modeling a linear transmission line with a resistive load in [5]. The system of differential equations can be written in conservation law form (1)

$$\frac{\partial \boldsymbol{u}}{\partial t} + \mathbf{A}\frac{\partial \boldsymbol{u}}{\partial x} = 0 \tag{13}$$

with

$$\boldsymbol{u} = \begin{pmatrix} i \\ v \end{pmatrix} \text{ and } \mathbf{A} = \begin{pmatrix} 0 & \frac{1}{L} \\ \frac{1}{C} & 0 \end{pmatrix}. \tag{14}$$

$\mathbf{A}$ is a matrix with constant coefficients in time and space, and its eigenvalues are found as

$$\lambda_1 = \frac{-1}{\sqrt{LC}} \text{ and } \lambda_2 = \frac{1}{\sqrt{LC}}. \tag{15}$$

The eigenvectors of the matrix $\mathbf{A}$ are

$$\boldsymbol{r}_1 = \begin{pmatrix} \sqrt{C} \\ -\sqrt{L} \end{pmatrix} \text{ and } \boldsymbol{r}_2 = \begin{pmatrix} \sqrt{C} \\ \sqrt{L} \end{pmatrix}. \tag{16}$$

referring to the two possible waves on the transmission line propagating in opposite directions. As an example, the propagation of a rectangular pulse was observed on a 1-m-long transmission line with a characteristic impedance of 50 Ω and a phase velocity of $c_0 = 3 \cdot 10^8$ m/s. To guaranty the stability of the numerical scheme, a Courant number

$$\nu = \left| \lambda_{1,2} \frac{\Delta t}{\Delta x} \right| \leq 1 \tag{17}$$

is required [2]. In this simulation, a Courant number ν of 0.5 was chosen. In Fig. 4, the resulting pulses on the transmission line of both the TVD and leapfrog scheme are compared after 1000 time steps. The total variation of the input signal $(\mathrm{TV}(u) = 2)$ is not increased by the TVD scheme, but strongly rises when using the leapfrog scheme. While the TVD scheme is able to model the discontinuities in the signal and does not flatten the slope significantly, the leapfrog scheme produces heavy oscillations, which make the result unusable.

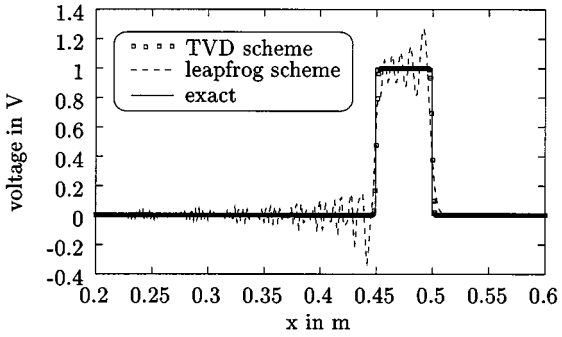

Fig. 4. Propagation of a rectangular pulse (0.167 ps) on a linear transmission line (50 Ω, $\beta = c_0$). Comparison between the leapfrog and TVD scheme after 1000 time steps. Courant–Friedrichs–Lewy number $= 0.5$.

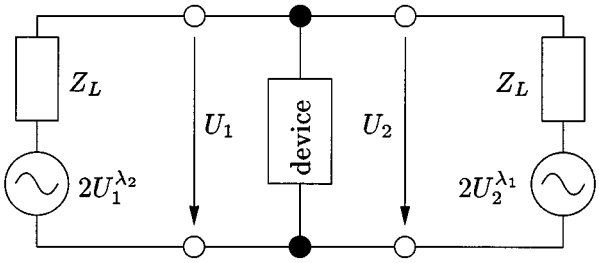

Fig. 5. Equivalent circuit for the computation of the scattering problem of the lumped element in the time domain.

Finally, the simulation times of the TVD and leapfrog schemes are compared. If, in both schemes, the same discretization in space and time is used, the computational effort of the TVD scheme is about ten times higher than that of the leapfrog scheme because the vector $\boldsymbol{u}$ has to be expanded in terms of the eigenvectors yielding more mathematical operations. Applying the leapfrog scheme to nearly discontinuous signals, however, the time step has to be decreased until the fall or rise time of the discontinuity is represented by at least 100 time steps, whereas in the TVD scheme, a jump in the signal can be characterized by only a few time steps or even by one time step.

IV. Inclusion of Lumped Elements

In the previous section, it has been shown that a TVD scheme is necessary if digital signals with short rise or fall times are used. However, even if a transmission-line network is excited with a smooth signal, steep edges can be caused by highly nonlinear lumped elements. As a consequence, the signal starts oscillating and leads to the same problems as discussed before. To analyze networks containing several lumped elements, a method for the inclusion of lumped elements in the transmission line has to be developed that is simultaneously preserving the TVD condition. The principle is based on a scattering problem in the time domain. In Fig. 5, the equivalent circuit of the problem is shown,

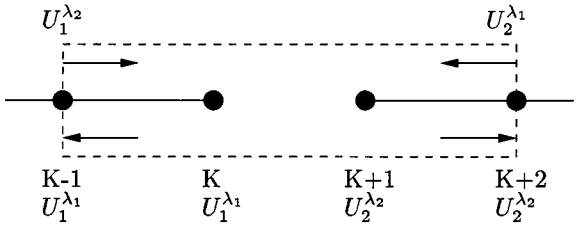

Fig. 6. Involved grid points belonging to the lumped element.

including the lumped element and voltage sources driven by the voltage of the incident wave at the time $n+1$. The voltages $U_1^{\lambda_2}|^{n+1}$ and $U_2^{\lambda_1}|^{n+1}$ are computed using the difference scheme at the grid points $K-1$ and $K+2$ (Fig. 6), respectively. Since $U_1^{\lambda_1}|_K$ and $U_2^{\lambda_2}|_{K+1}$ are set to zero, no reflected wave is excited and, therefore, an ABC at the grid nodes $K-1$ and $K+2$ is obtained. The ABC is, at most, first-order accurate and depends mainly on the values for $U_1^{\lambda_2}|_K$ and $U_2^{\lambda_1}|_{K+1}$, which influence the accuracy but do not affect the reflection coefficient $\Gamma_{\mathrm{ABC}}=0$. The implementation of the ABC becomes possible in such a way because the TVD scheme is based on condensed nodes where the vector $\boldsymbol{u}$ can be decomposed in terms of eigenvectors.

From the equivalent circuit (Fig. 5), a system of the differential equation

$$\mathbf{A}\frac{\partial \boldsymbol{X}}{\partial t}+\mathbf{B}(\boldsymbol{X})=0 \tag{18}$$

results, which has to be solved for the time step $n \rightarrow n+1$, where the state vector $\boldsymbol{X}$ contains the voltages and currents of the network. Applying the backward Euler method, (18) can be approximated by the difference equation

$$\mathbf{A}\left(\boldsymbol{X}^{n+1}-\boldsymbol{X}^{n}\right)+\mathbf{B}\left(\boldsymbol{X}^{n+1}\right)=0 \tag{19}$$

and the resulting nonlinear system of equations can be solved with the Newton method. Next, on both ports, the voltages and currents of the scattered waves are extracted from the state vector $\mathbf{X}^{n+1}$ and can finally be updated on all four grid points (Fig. 6) at the time step $n+1$. At the time step $n+1$, the voltage of the reflected wave at both ports ($K-1$ and $K+2$) is finally given by

$$U_1^{\lambda_1}|^{n+1}=U_1|^{n+1}-U_1^{\lambda_2}|^{n+1} \tag{20}$$

and

$$U_2^{\lambda_2}|^{n+1}=U_2|^{n+1}-U_2^{\lambda_1}|^{n+1}. \tag{21}$$

As an example, a diode with an ideal characteristic

$$I=I_0\left(\mathrm{e}^{U/U_t}-1\right) \tag{22}$$

with $I_0=1$ mA and $U_T=25$ mV is included in the middle of the transmission line with a characteristic impedance of 50 Ω and a phase velocity of $3\cdot 10^8$ m/s. The voltage distribution

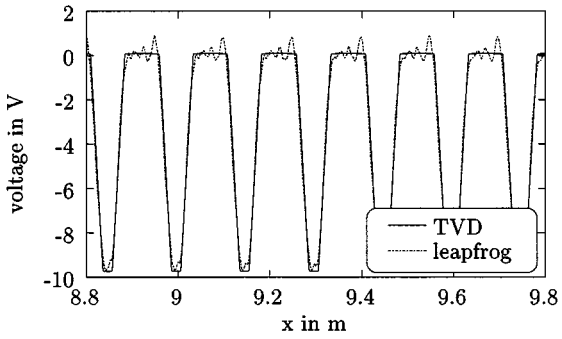

Fig. 7. Propagation of a scattered harmonic signal (2 GHz) on a 10-m-long transmission line (50 Ω, $\beta=c_0$) loaded with a diode placed in the middle of the line after 20 000 time steps (Courant number $=0.5$).

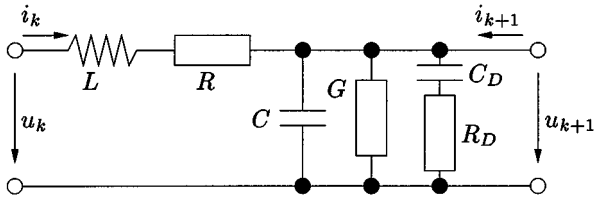

Fig. 8. Model of an NLTL.

along a section at the end of the 10-m-long transmission line is shown in Fig. 7 after 20 000 time steps.

The circuit was excited with a harmonic signal with an amplitude of 10 V and a frequency of 2 GHz. Due to the strongly nonlinear characteristic of the diode, steep edges occur in the time signal, and the signal computed with the leapfrog method starts oscillating while propagating on the transmission line.

V. NLTL

In this section, the second-order TVD scheme is applied to an NLTL with distributed diodes according to Fig. 8. With such a scheme, the formation of shock waves can be simulated without spurious oscillations caused by non-TVD schemes. Since the losses of the NLTL are very low, the resistance R, conductance G, and resistance of the diode R_D per length can be neglected and set to zero. Using the charge q instead of the voltage u for the second variable, the charge can be expressed by

$$q=Cu+Q_D(u)=g(u) \tag{23}$$

where $Q_D(u)$ is the voltage-dependent charge per length of the diode, and C is the capacitance per length of the linear transmission line. The charge $Q_D(u)$ is obtained by an integration of the capacitance $C_D(u)$ over the voltage u. The system of conservation laws can be written analogously to the linear transmission line in Section III as

$$\begin{pmatrix} i \\ q \end{pmatrix}_t+\begin{pmatrix} \frac{g^{-1}(q)}{L} \\ i \end{pmatrix}_x=0. \tag{24}$$

In the nonlinear case, the eigenvalues

$$\lambda_1=\frac{-1}{\sqrt{L\frac{\partial}{\partial u}g\left(g^{-1}(\hat{q})\right)}}\quad \lambda_2=-\lambda_1 \tag{25}$$

TABLE I
ELECTRICAL PROPERTIES OF THE GAAS NLTL

L in nH/m	C in pF/m	C_{j0} pF/m	U_D in V
588	132	288	0.7

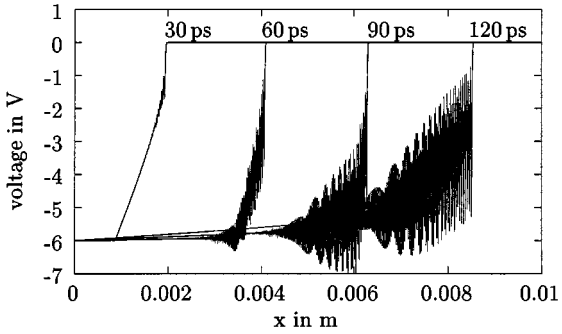

Fig. 9. Shock formation on the GaAs NLTL excited with a step function with 20-ps fall time; signal on the NLTL after 30, 60, 90, and 120 ps using leapfog scheme.

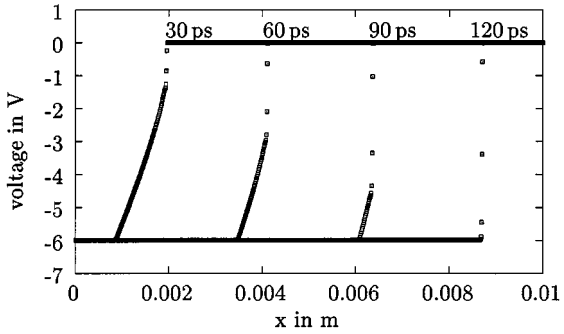

Fig. 10. Shock formation on the GaAs NLTL excited with a step function with 20-ps fall time; signal on the NLTL after 30, 60, 90, and 120 ps using the TVD scheme.

and eigenvectors

$$\boldsymbol{r}_1 = \begin{pmatrix} 1 \\ -\sqrt{L\frac{\partial}{\partial u}g\big(g^{-1}(\hat{q})\big)} \end{pmatrix} \quad \boldsymbol{r}_2 = \begin{pmatrix} r_{11} \\ -r_{12} \end{pmatrix} \tag{26}$$

depend on both space and time and, consequently, have to be computed for each grid point and each time step. $\hat{q}$ is a kind of average between q_{k+1}^n and q_k^n and has to be determined so that the three conditions for the Jacobian matrix $\hat{\mathbf{A}}$ of Section II are fulfilled. To this end, $\hat{q}$ has to satisfy

$$\frac{\partial}{\partial u}g\big(g^{-1}(\hat{q})\big) = \frac{q_{k+1}^n - q_k^n}{g^{-1}\Big(q_{k+1}^n\Big) - g^{-1}\Big(q_k^n\Big)}. \tag{27}$$

As a numerical example, the GaAs NLTL presented in [9] is used for a comparison between the TVD and leapfrog schemes. The electrical properties of the NLTL are listed in Table I. Since a homogeneous doping profile for the diodes is chosen, the capacitance per length is given by

$$C_D(u) = \frac{C_{j0}}{\sqrt{1 - \frac{u}{U_D}}}. \tag{28}$$

The 1-cm-long NLTL was excited by a step function with a fall time of 20 ps. In Figs. 9 and 10, the voltage on the NLTL is shown after 30, 60, 90, and 120 ps. Using the TVD scheme, the voltage jumps from 0 to -6 V within a few space steps at the shock. With the leapfrog scheme, heavy oscillations occur when the partial shock arises and, after 70 ps, the signal is unusable for further studies.

The propagation velocity of the shock

$$v_{\text{shock}} = \frac{1}{\sqrt{L\dfrac{q_R - q_L}{g^{-1}(q_R) - g^{-1}(q_L)}}} \tag{29}$$

can also be accurately modeled by the TVD scheme. To this end, an analysis of NLTLs requires a numerical scheme that is conservative and TVD. Even if losses are introduced in the NLTL, such a scheme has to be taken if the fall time comes into the range of several time steps ($< 100\,\Delta t$) or space steps.

VI. CONCLUSION

In this paper, the TVD algorithm has been introduced for the finite-difference solutions of nonlinear transient electromagnetic-wave problems. As an example of higher resolution schemes, a second-order TVD scheme based on the Lax–Wendroff scheme was applied to a linear transmission line loaded with a nonlinearity and to a low-loss NLTL. It has be shown that the commonly used leapfrog scheme fails when dealing with highly nonlinear low-loss structures. In this paper, only the application to the 1-D problem was shown. Further work is being carried out for more challenging work in the two-dimensional (2-D) or 3-D case in electromagnetics.

REFERENCES

[1] P. Ciampolini, P. Mezzanotte, L. Roselli, and R. Sorrentino, "Accurate and efficient circuit simulation with lumped-element FDTD technique," *IEEE Trans. Microwave Theory Tech.*, vol. 44, pp. 2207–2214, Dec. 1996.

[2] J. W. Thomas, *Numerical Partial Differential Equations, Conservation Laws and Elliptic Equations*. New York: Springer-Verlag, 1999.

[3] ——, *Numerical Partial Differential Equations, Finite Difference Methods*. New York: Springer-Verlag, 1995.

[4] D. Koerner, *Numerical Schemes for Conservation Laws*. New York: Wiley, 1997.

[5] K. -P. Hwang and J. Jian-Ming, "A total-variation-diminishing finite difference scheme for a transient response of a lossless transmission line," *IEEE Trans. Microwave Theory Tech.*, vol. 46, pp. 1193–1196, Aug. 1998.

[6] P. L. Roe, "Approximate Riemann solvers, parameter vectors and difference schemes," *J. Comput. Phys.*, vol. 43, pp. 357–372, 1981.

[7] ——, "Some contributions to the modeling of discontinuous flows," *Lecture Notes Appl. Math.*, vol. 22, p. 163, 1985.

[8] K. S. Yee, "Numerical solution of initial boundary value problems involving Maxwell's equation in isotropic media," *IEEE Trans. Antennas Propagat.*, vol. 14, pp. 302–307, May 1966.

[9] A. Jrad, W. Thiel, P. Ferrari, and J. W. Tao, "FDTD and SPICE simulations for lossy and dispersive nonlinear transmission lines used for pulse compression: a comparison," in *Proc. 30th European Microwave Conf.*, 2000, pp. 264–267.

[10] R. Huelsewede, U. Effing, I. Wolff, and D. Jaeger, "CAD of pulse compression on nonlinear transmission lines," in *German Microwave Conf. (MIOP)*, 1995, pp. 511–515.

Werner Thiel was born in Altötting, Germany, in 1970. He received the Dipl.-Ing. and Dr.-Ing. degrees from the University of Ulm, Ulm, Germany, in 1995 and 2000, respectively.

From 1995 to 2001, he was with the Microwave Techniques Department, University of Ulm. Since April 2001, he has been with the Department of Electrical Engineering, Radiation Laboratory, The University of Michigan at Ann Arbor. His research activities and interests include finite-difference techniques in general, development of finite-difference time-domain (FDTD) software, and the design and optimization of nonlinear components in millimeter waves applying the FDTD method.

Wolfgang Menzel (M'89–SM'90–F'01) received the Dipl.-Ing. degree from the Technical University of Aachen, Aachen, Germany, in 1974, and the Dr.-Ing. degree from the University of Duisburg, Duisburg, Germany, in 1977.

From 1979 to 1989, he was with the Millimeter-Wave Department, AEG (now EADS), Ulm, Germany. From 1980 to 1985, he was Head of the Laboratory for Integrated Millimeter-Wave Circuits. From 1985 to 1989, he was Head of the Millimeter-Wave Department. During that time, his areas of interest included planar antennas, and planar integrated circuits and systems in the millimeter-wave frequency range. In 1989, he became a Full Professorship at the University of Ulm, Ulm, Germany. His current areas of interest are (multilayer) planar and waveguide circuits, antennas, millimeter-wave interconnects and packaging, and millimeter-wave system aspects.